

List of Figures

Figure 1: Sample conformations of GV4 separated into three categories based on their end-to-end distance. Hairpin and hairpin-like conformations are shown in the left panel; turns and turn-like conformations are in the center panel; and the right panel contains extended conformations.

Figure 13. Snapshots of Simulation C after 219 ns of simulation time. The top side of the slab (left) shows more ordered β -structures than the right side. Both sides show extended dimers, trimers, or other larger structures. The peptides are shown with valines in pink, glycines in a different color depending on the chain. The octane slab is shown in white.

Figure 14. Timescale of aggregation for one run from Simulation B2. a) 12 ns. b) 14 ns. c) 20 ns. d) 26 ns. Valines are colored in pink, glycines are colored using a different color for each chain. The slab is shown in white.

Figure 15. One run in Simulation D, after 160 ns of additional simulation time, showing a large globular aggregate. Color is similar to that in Figure 14.

Figure 1: Simulation snapshots showing adsorption of one chain to the octane surface. a) Adsorption is initiated by interaction between at least one valine side chain (shown in pink) and the octane slab (shown in blue) at 1.5 ns. b) After 6 ns, the peptide is lying flat on the slab, and has taken on an extended conformation.

Figure 2: Proportion of GV4 chains remaining fully solvated over the timescourse of Simulation B1. Fitted with an exponential fit.

Figure 3: Densities and distributions of various atoms with the interface. a) Density profile for Simulation C2 showing distribution of backbone, $C\alpha$, and Val $C\gamma$ atoms. b) Axial distribution of valine $C\gamma$ atoms and $C\alpha$ atoms normalized with respect to the slab surface.

Figure 4: The number of waters in the first hydration shell of the $C\gamma$ atoms compared to the number of backbone bound waters. a) Simulation A; b) Simulation D; c) Simulation B1; d) Simulation B2; e) Simulation C1; f) Simulation C2. A progressive increase in dehydration is seen in panels (c) through (f).

Part C: End-to-end distance effects of slab binding

Figure 5: Normalized distribution of d_{ete} . Simulations on the slab are listed at the top, in order of increasing timescale and concentration. Simulations in water are shown at the bottom. Y axis is arbitrary. For simulations on the slab, the plateau (> 2 nm) grows and the hairpin conformation (centered at ~ 0.66 nm) becomes less prevalent over time, both effects not observed in water. Standard error is depicted as shading around the lines.

Figure 6: Time-evolution of d_{ete} for simulations B1 and B2. Note that most of the extension occurs in the first 10 ns, the bulk of the exchange appears between the intermediate (0.66 – 1.30

nm) and extended conformations (> 1.30 nm). There is a marked exchange between the intermediate and extended conformations.

Figure 7: Ratios of closed, intermediate and extended conformers in simulations. Systems in a) are on the slab, systems in b) are in water. Simulation A is included as a control in (b) for comparison.

Part D: Hydrogen bonding

Figure 8: Hydrogen bond time evolution. a) Simulation B1 and B2. Note the linear increase for the first 6 ns, followed by an increase at a slower rate. b) Simulation C1 and C2. At high concentration and longer time-scales the number of intermolecular hydrogen bonds formed between the chains keeps increasing gradually after an initial surge of formation of new bonds and is far greater than that of the intramolecular bonds, which maintain a baseline level of ~ 0.5 bonds / chain. c) Simulation D. A very rapid initial increase in intermolecular hydrogen bonds is apparent, which tapers off after the initial aggregation occurs.

Figure 9: d_{ete} distribution, separated by type of hydrogen bonding. a) Simulation B2: There is a slight plateau at $d_{ete} > 2$ nm for peptides with only intermolecular bonds, compared to those with no hydrogen bonds. The peptides with both inter-peptide and intra-peptide hydrogen bonds or intramolecular bonds only remain in more closed conformations in comparison to all other peptide chains. b) Simulation C2. Over a longer time-scale at high concentrations, there is a separation between the distance distributions of peptides without any hydrogen bonds and those with only intermolecular bonds. The plateau at 2 nm or greater is larger in size than for Simulation B2. c) Simulation D. The overall separation is similar to that with the slab systems. However, more of the peptides that have either intermolecular hydrogen bonds or have no hydrogen bonds are in the lower range of the distance spectrum. Standard error is represented by the shaded regions around the lines.

Part E: Aggregates

Figure 10: Timescale of aggregation. a) Aggregation for Simulations B1 and B2. b) Aggregation for Simulation C1 and C2.

Figure 11. Hydrogen bonding, separated by type and number of hydrogen bonds, compared to backbone bound waters.

Part F: Secondary Structure

Figure 12: Secondary structure time evolution of GV4 systems. a) B1 and B2. b) C1 and C2. The beta sheets increase linearly for the first 5-6 ns, after which they begin increasing in a slower rate.

Figure 1

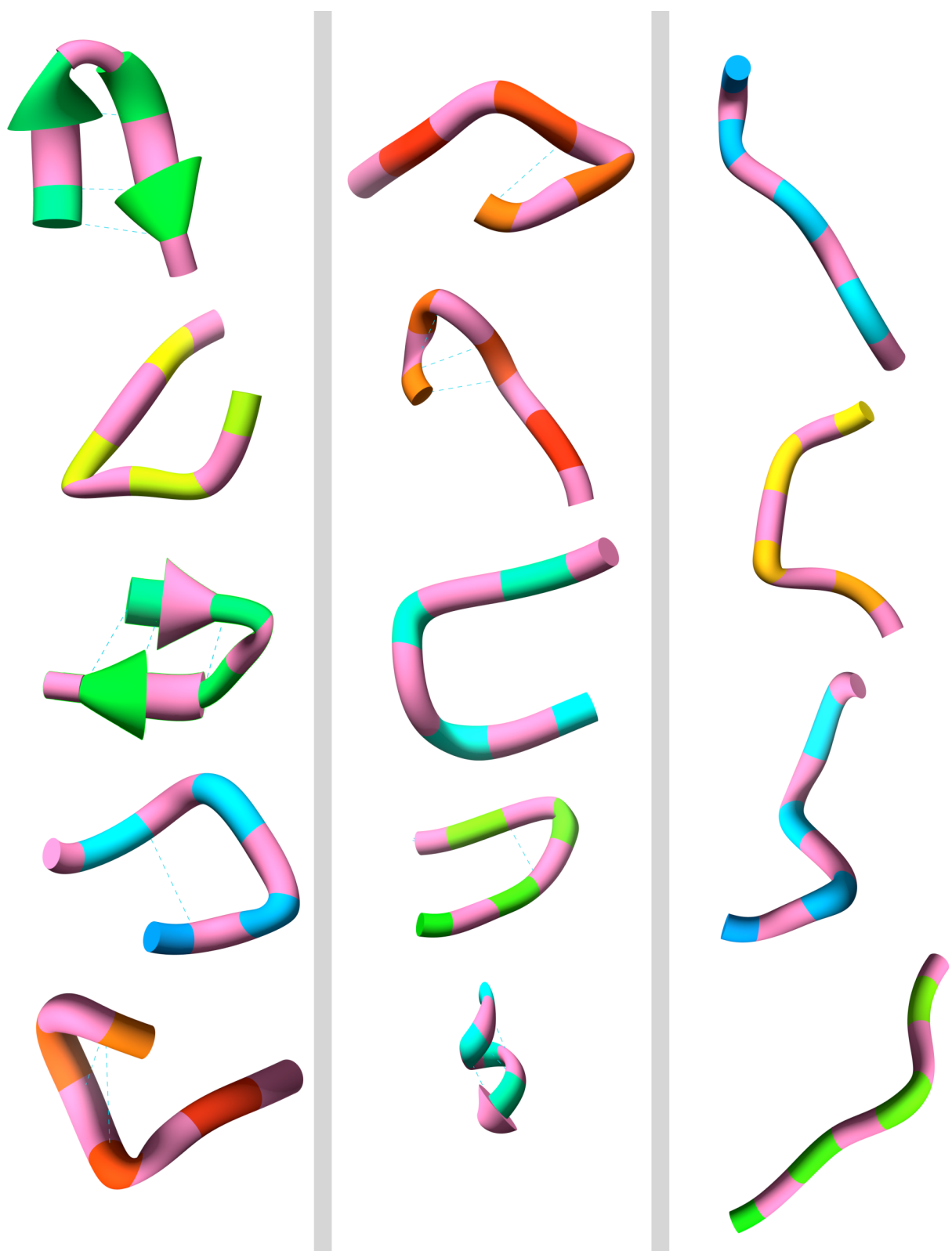


Figure 13

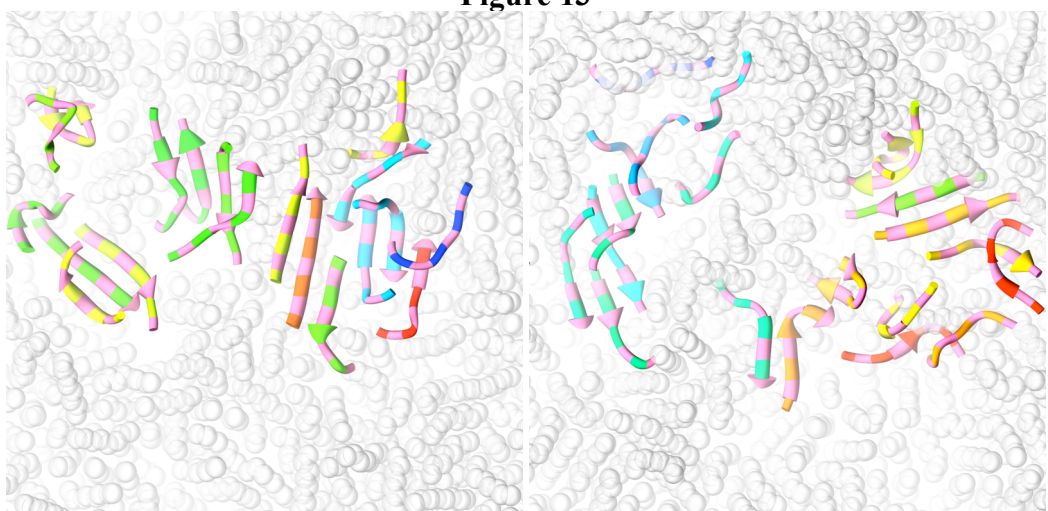


Figure 14

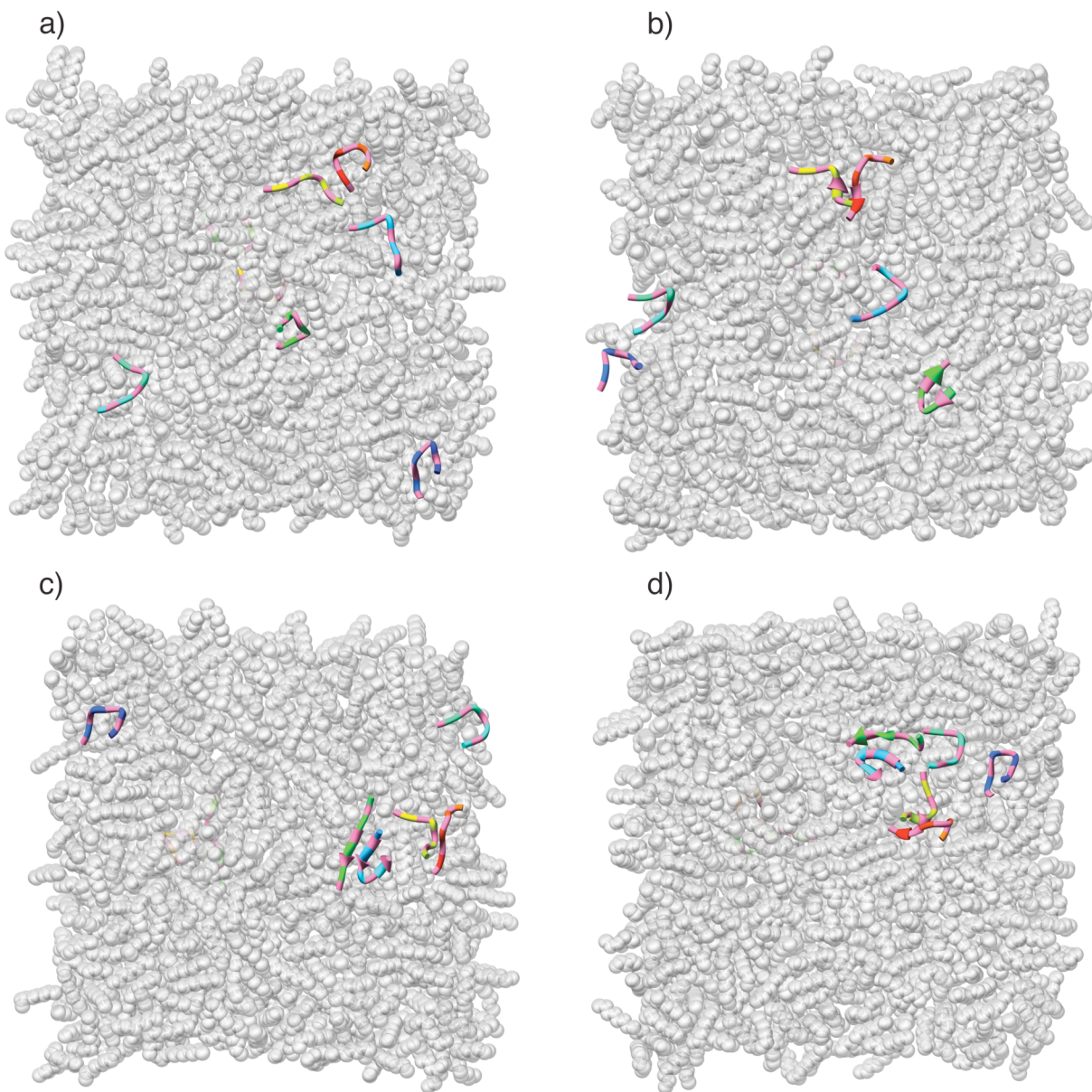


Figure 15

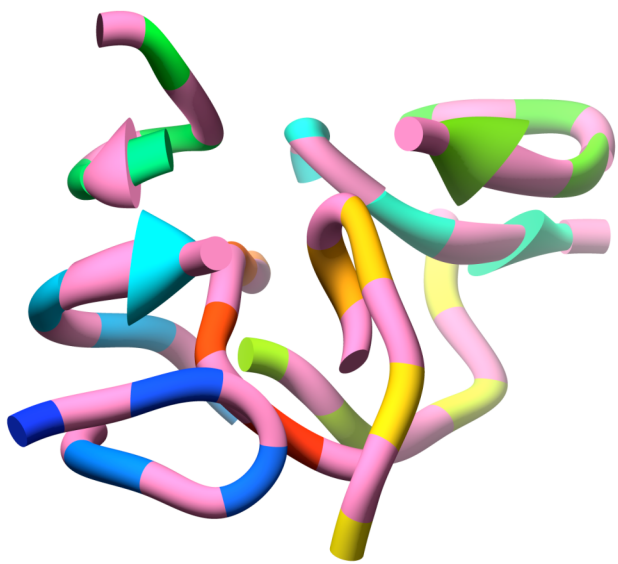
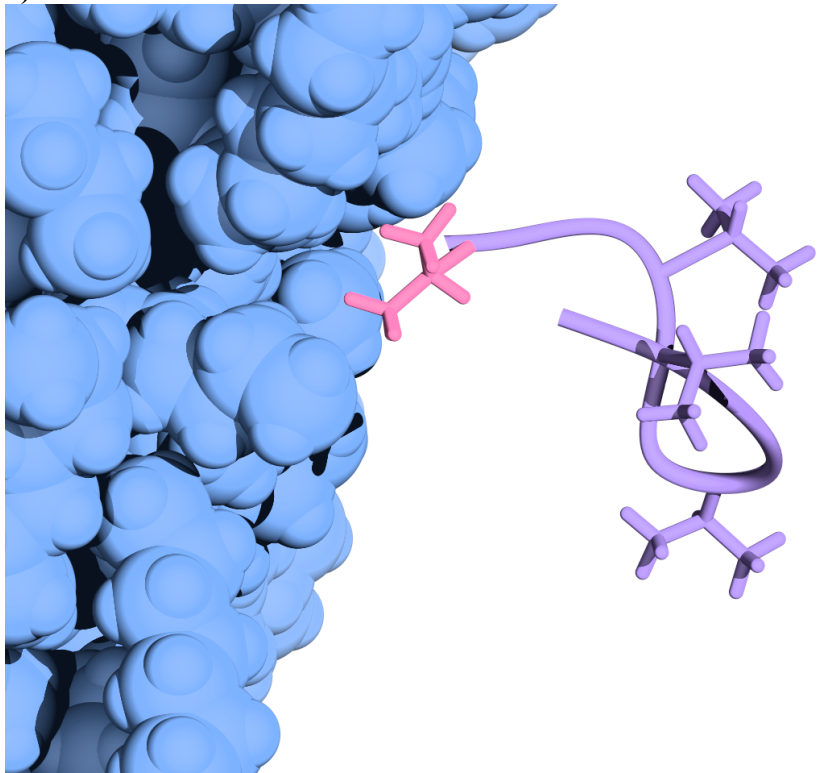


Figure 1

a) 1.5 ns



b) 6.5 ns

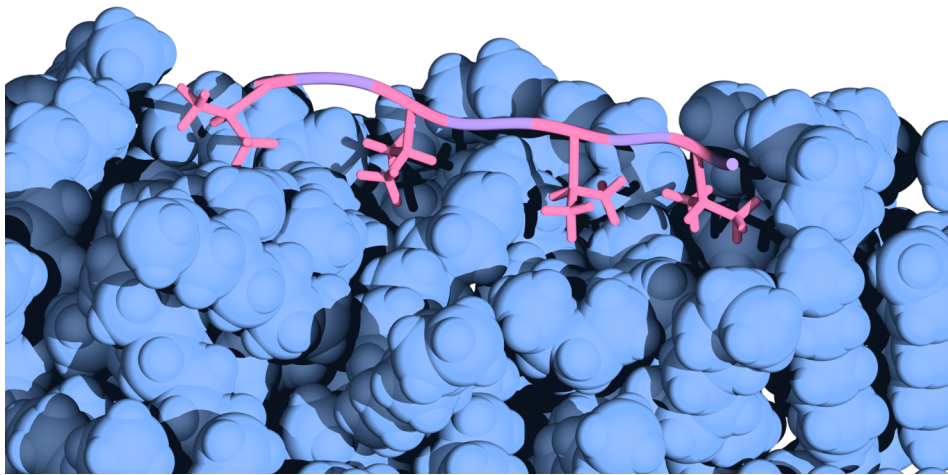


Figure 2

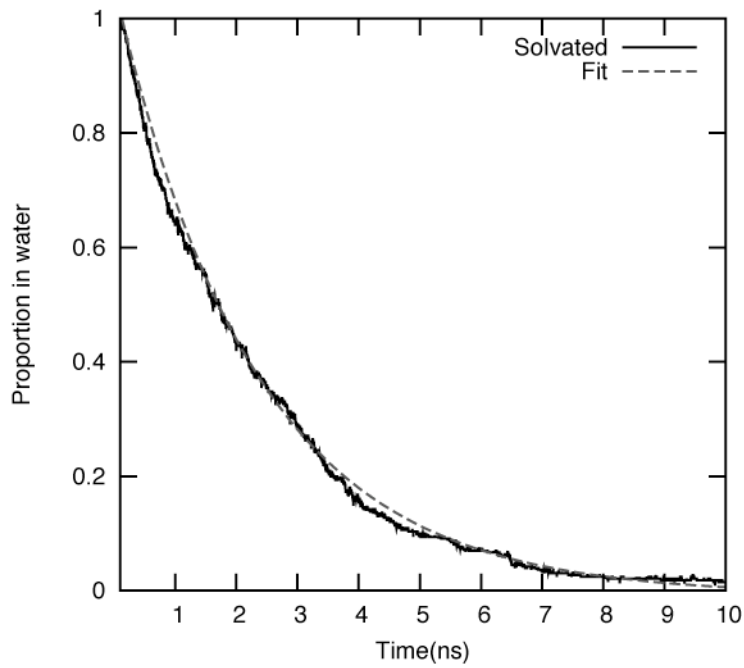
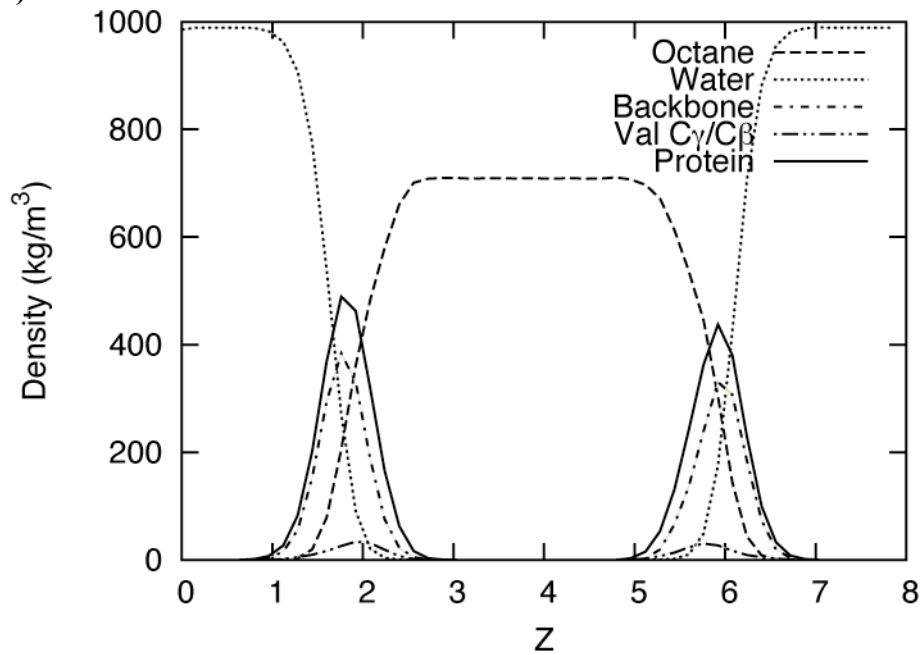


Figure 3

a)



b)

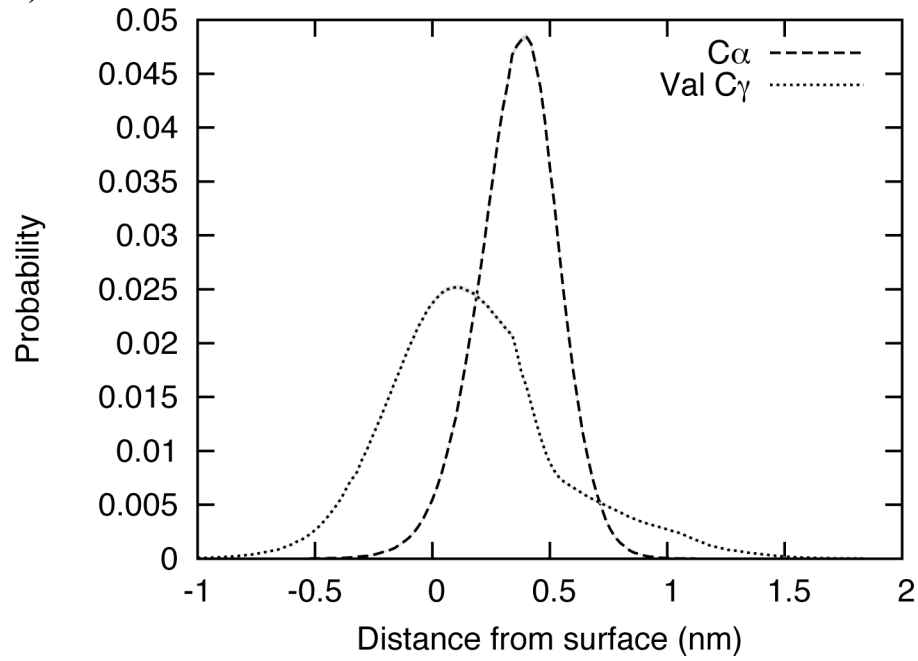


Figure 4

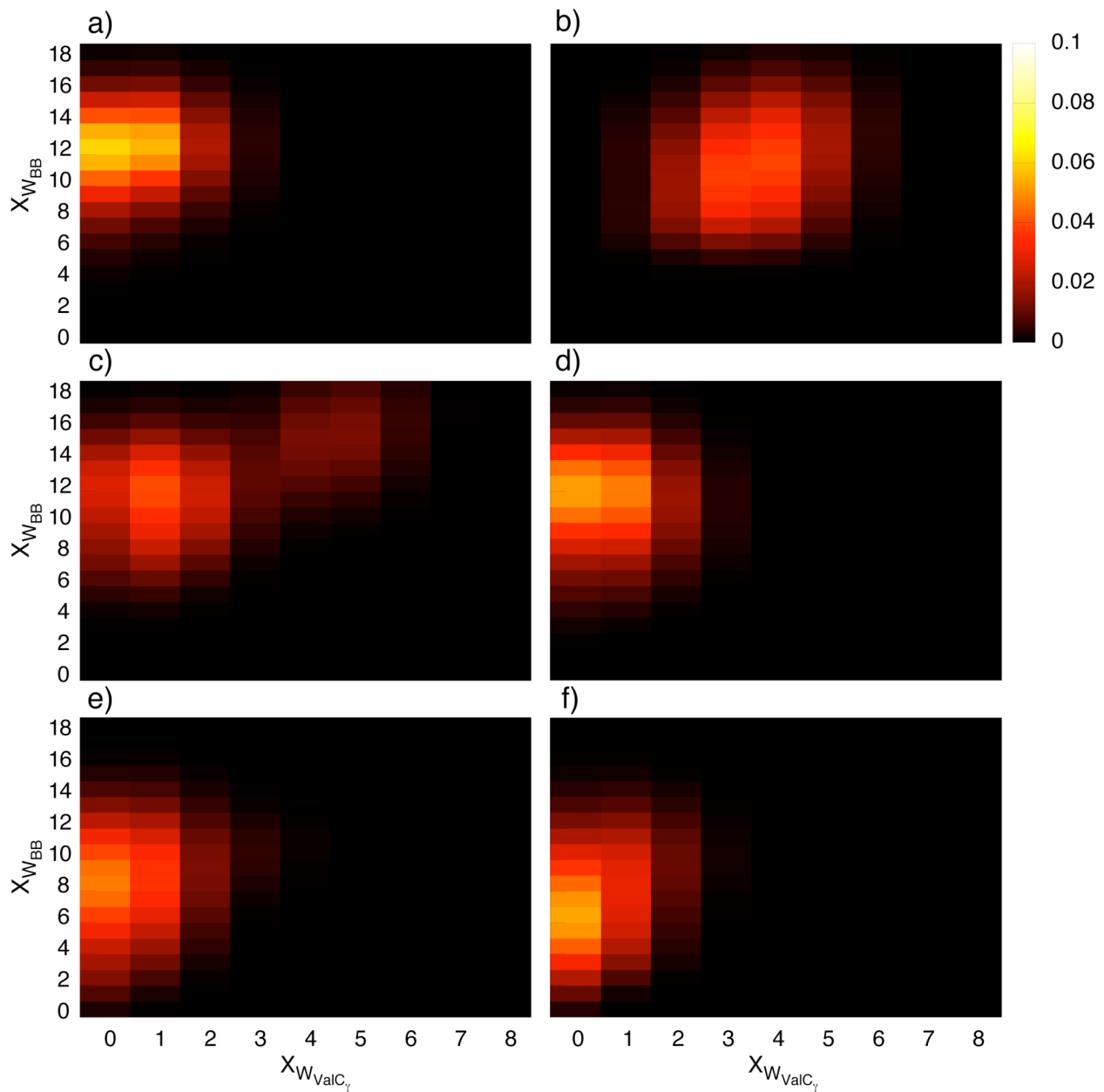


Figure 5

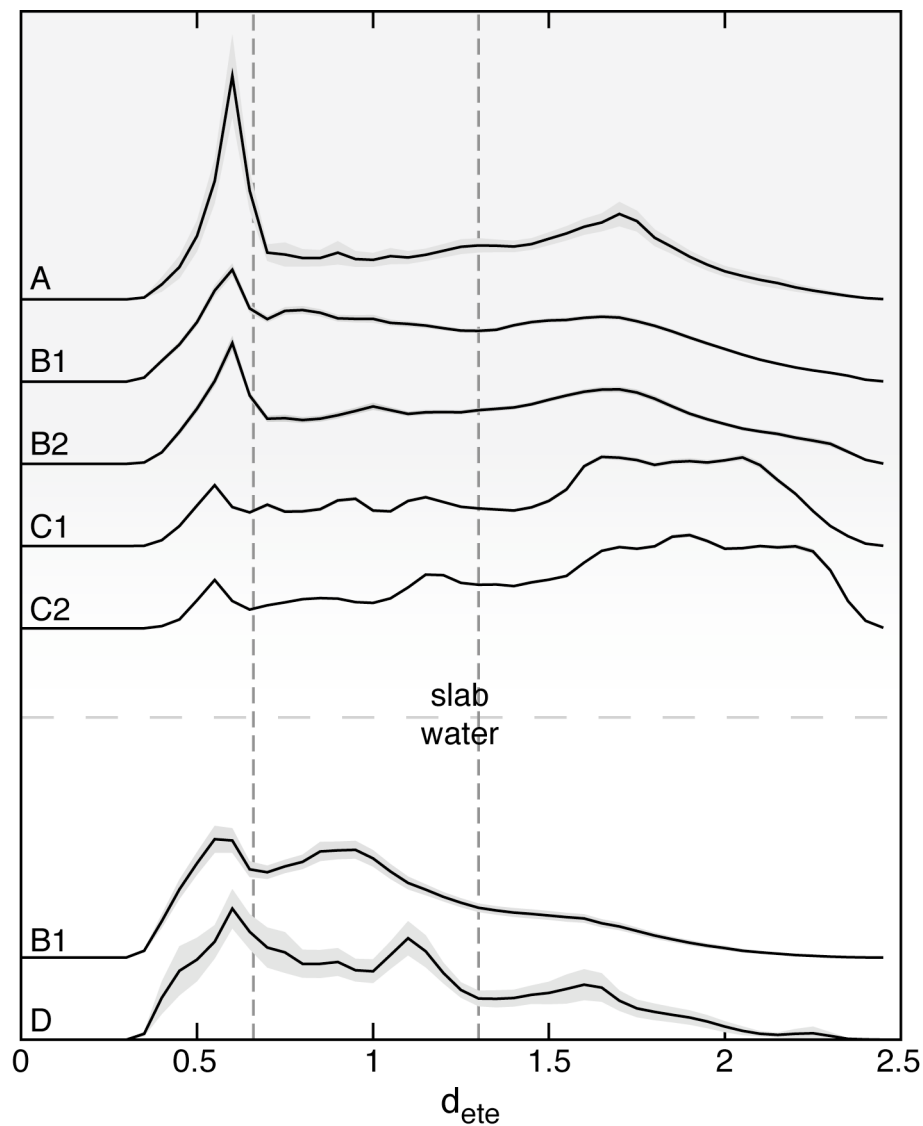


Figure 6

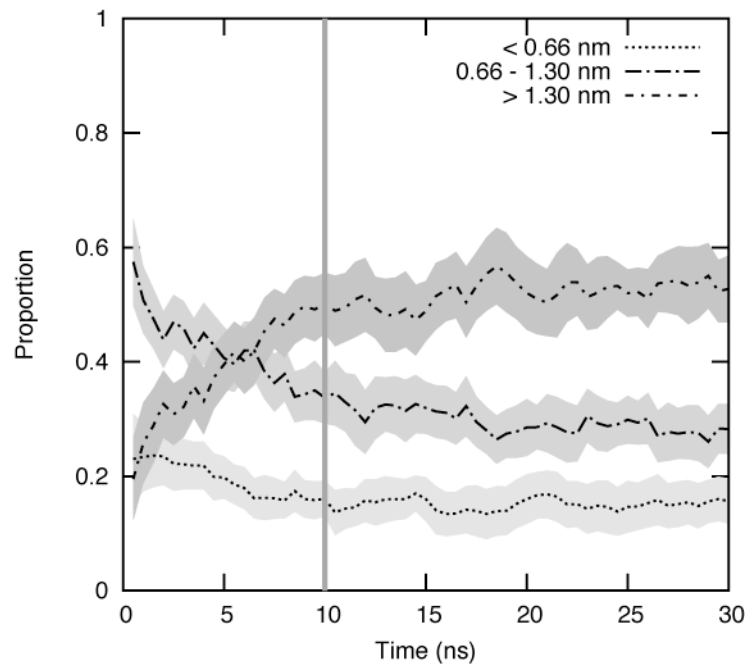


Figure 7

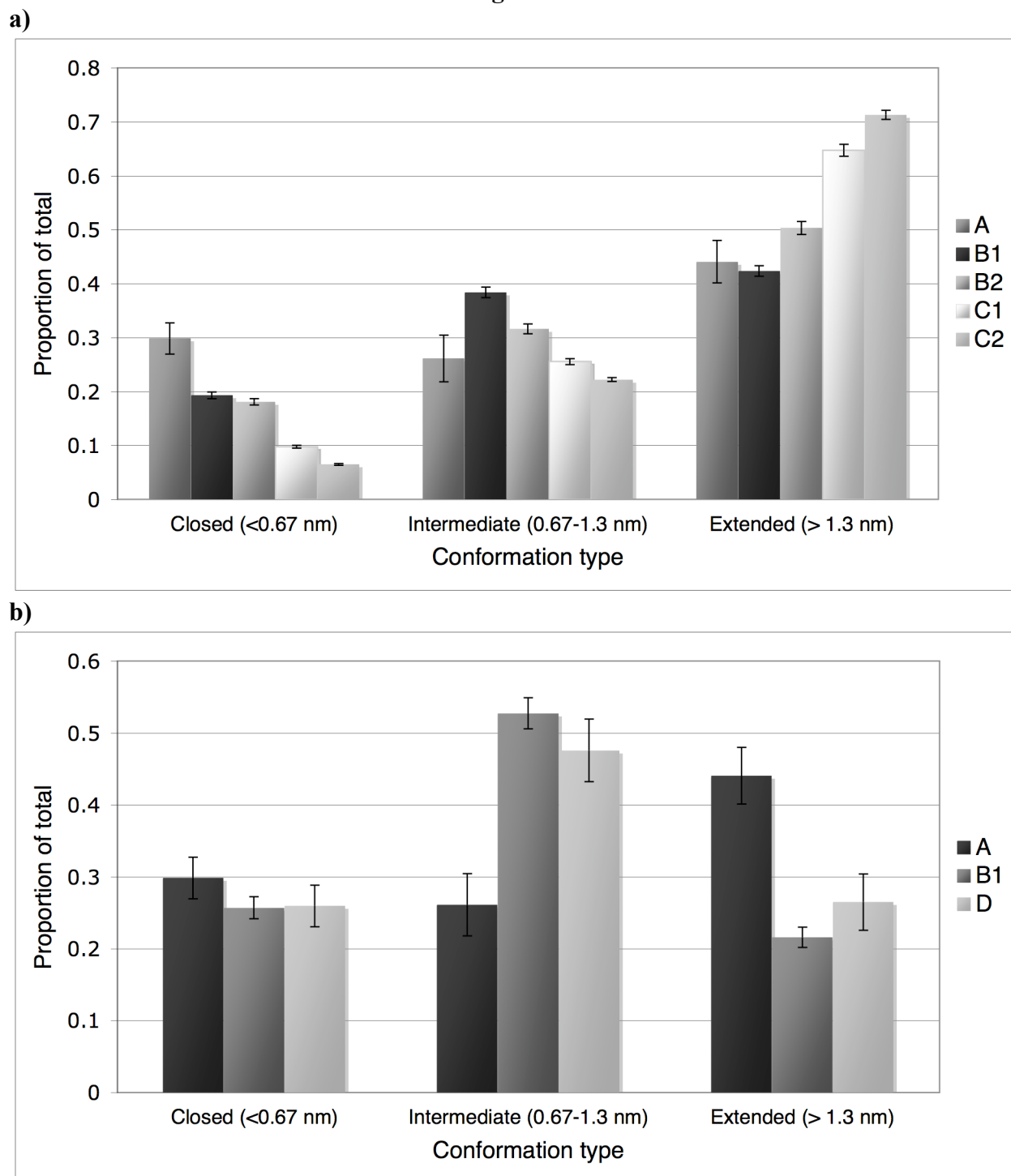
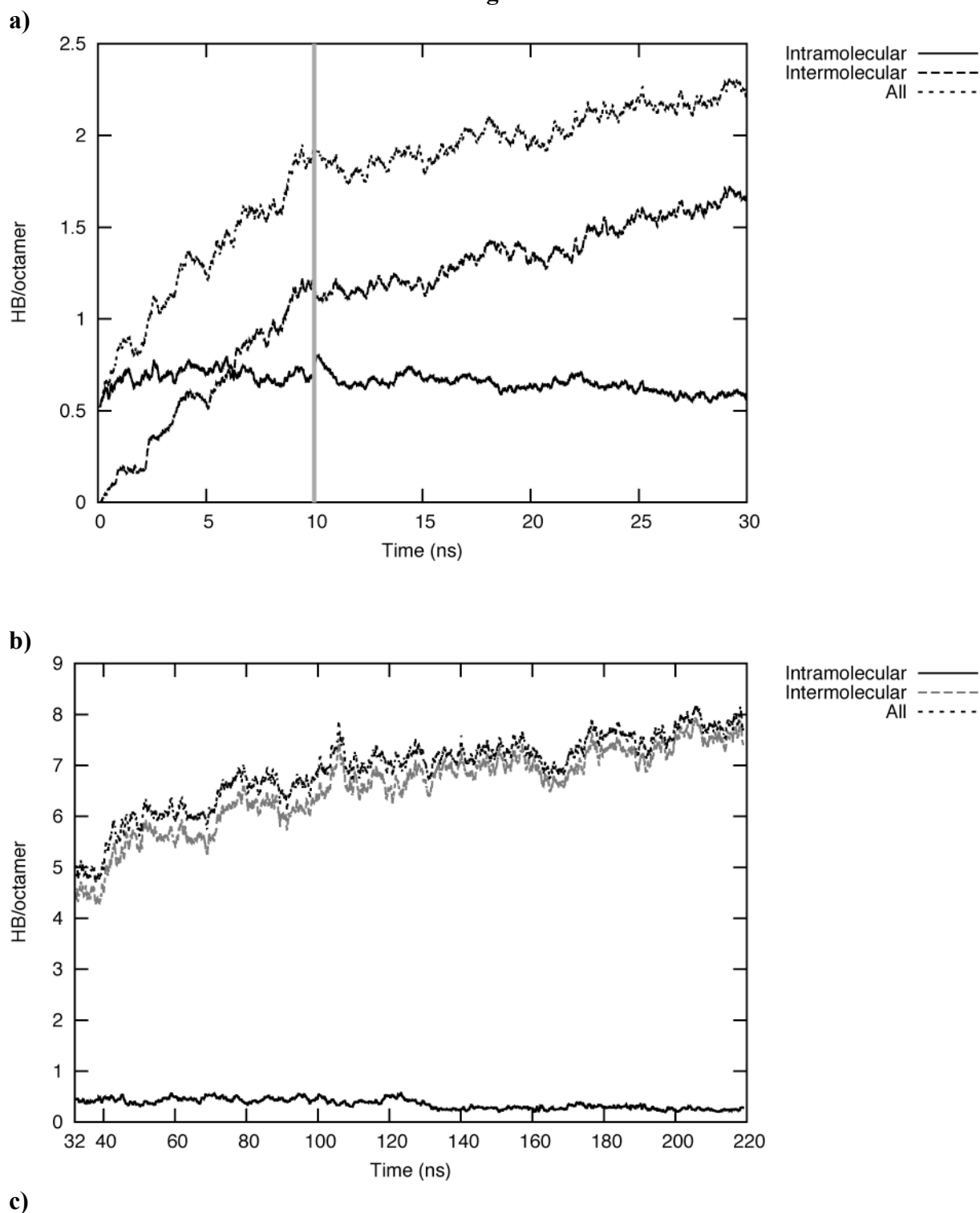


Figure 8



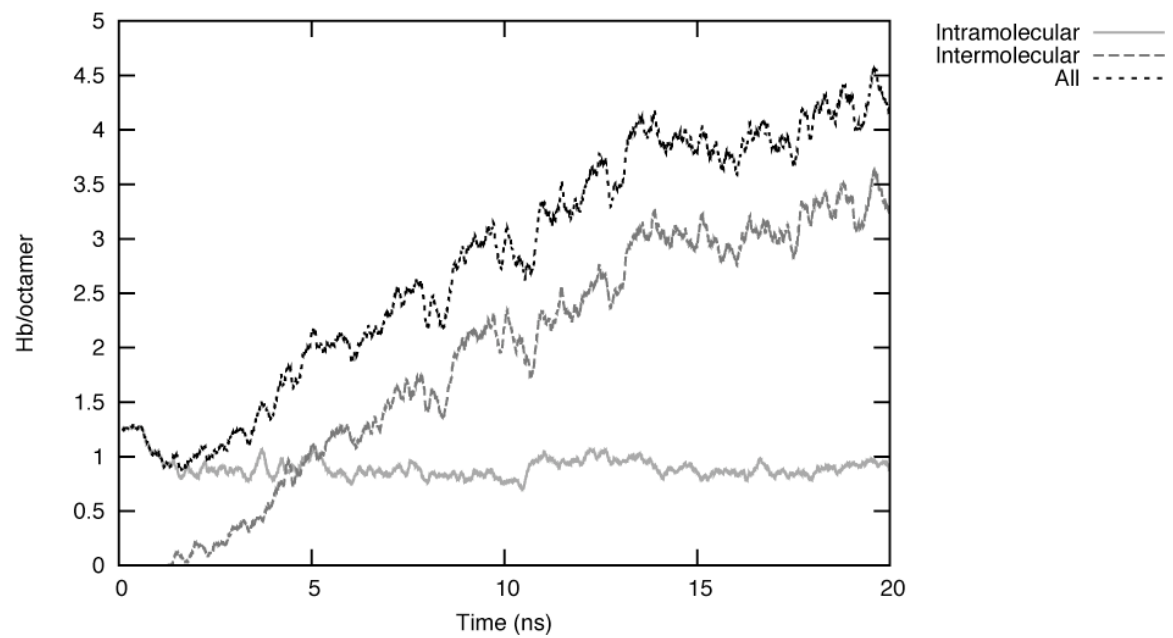
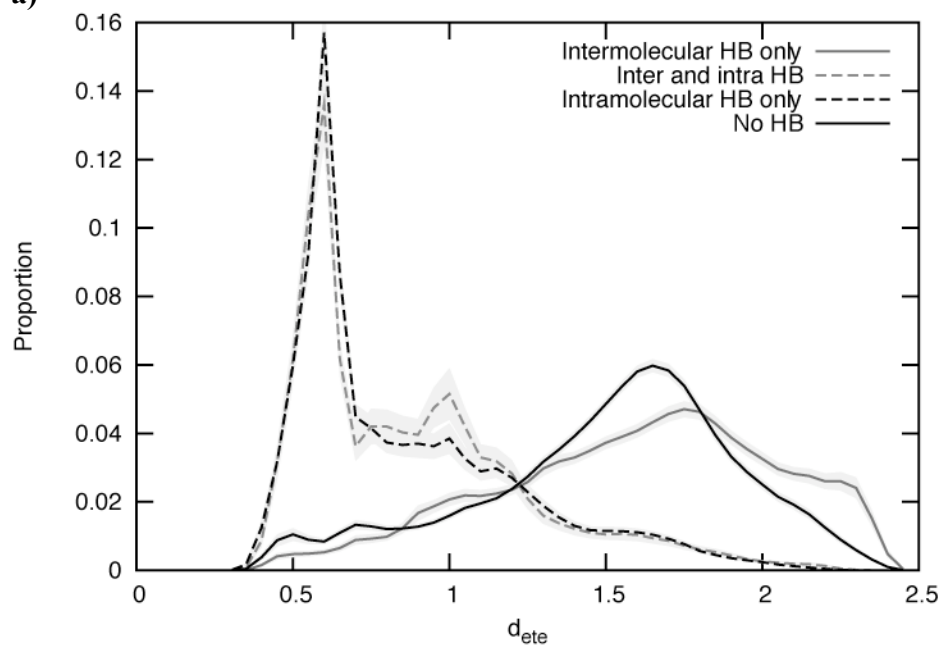
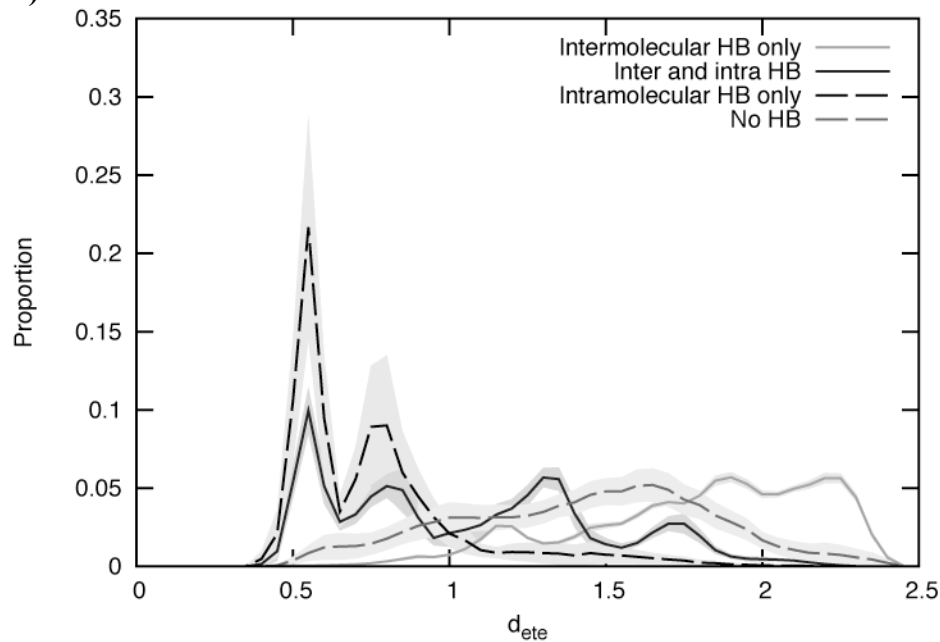


Figure 9**a)****b)****c)**

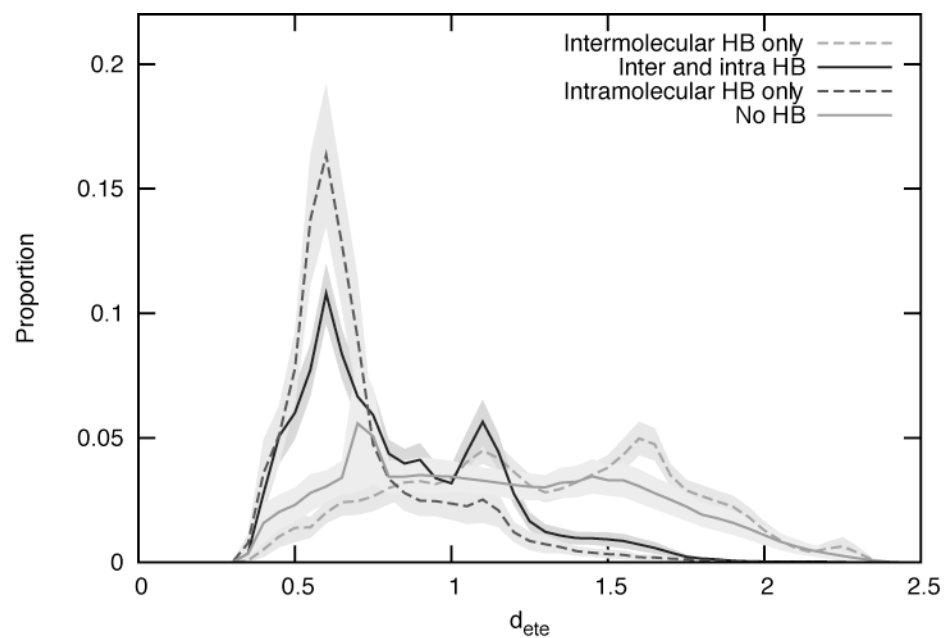


Figure 10

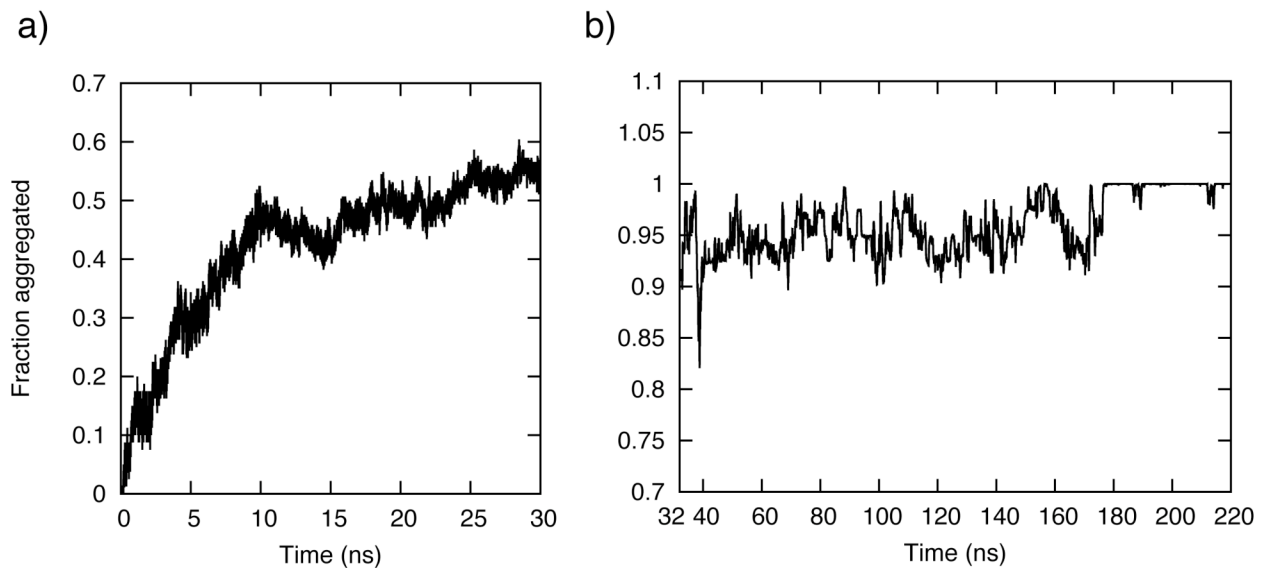


Figure 11

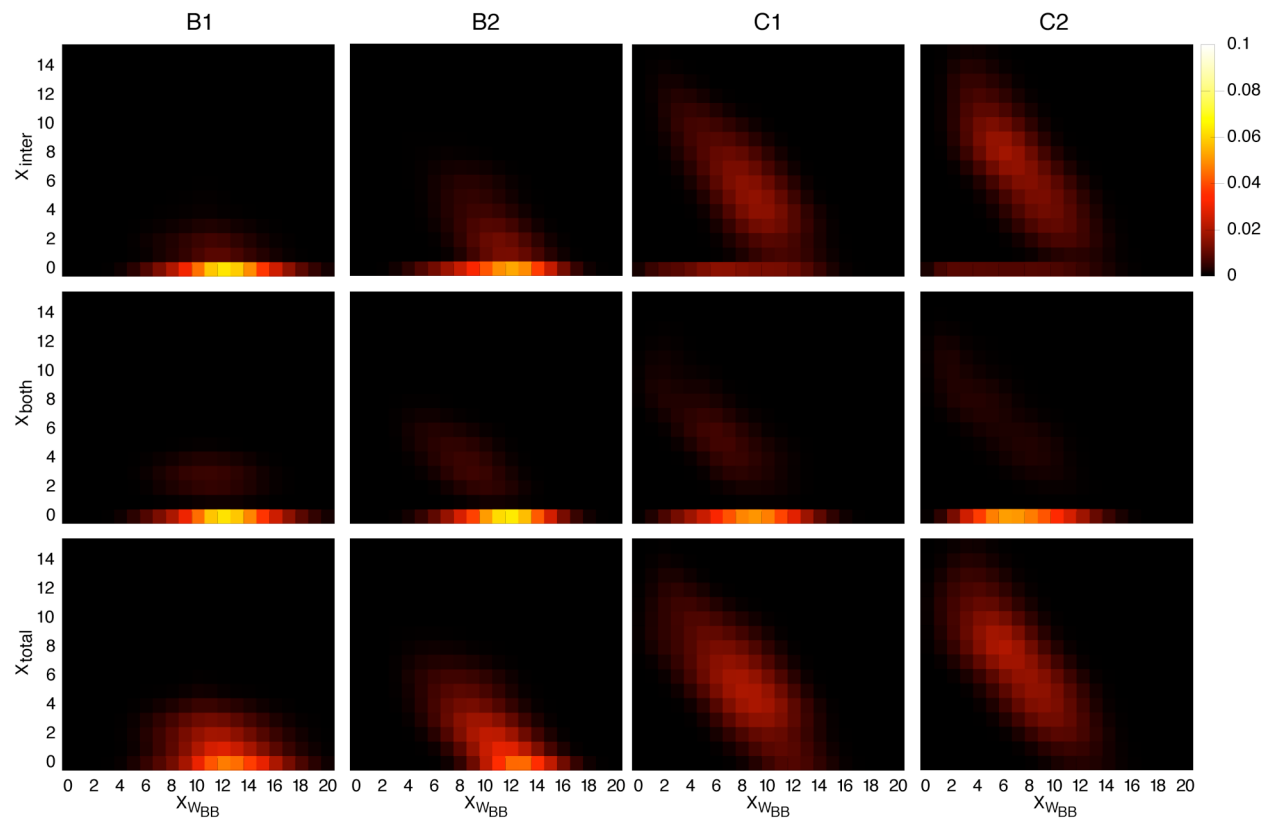
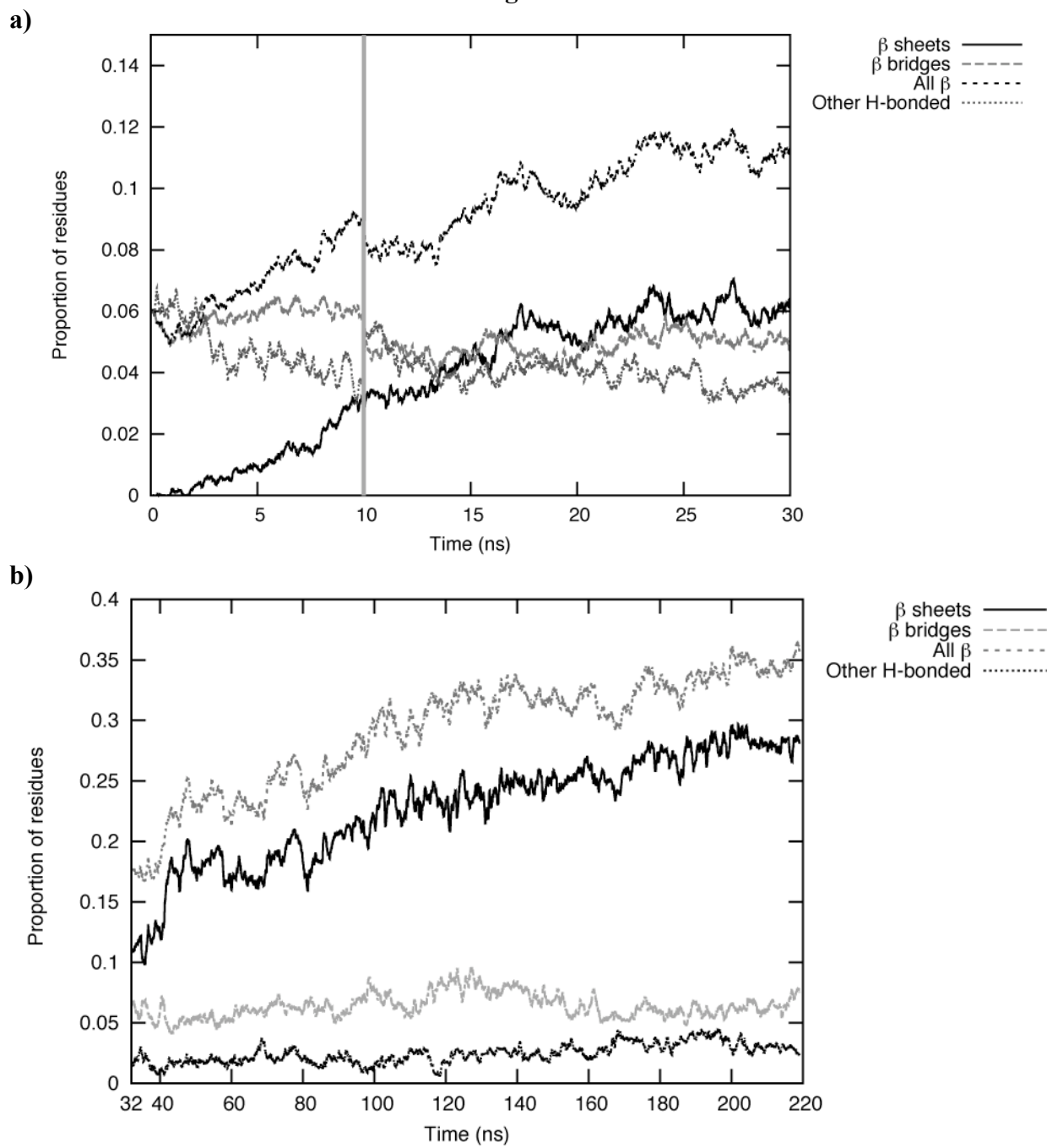


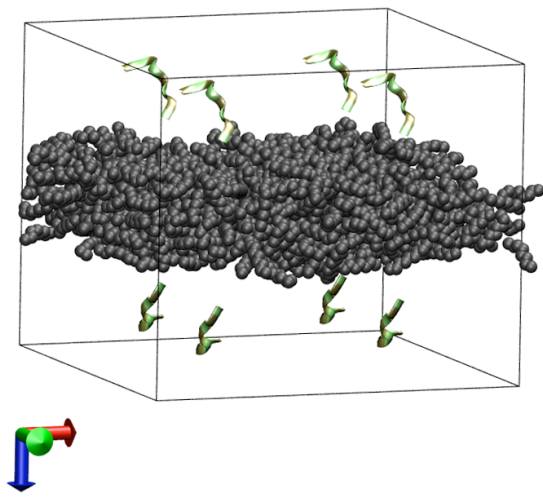
Figure 12



Other pictures:

- 1) representative starting structure (for Simulation B1) [supplementary]

Side view



Top view

